



# The Change of Teleost Skin Commensal Microbiota Is Associated With Skin Mucosal Transcriptomic Responses During Parasitic Infection by *Ichthyophthirius multifiliis*

Xiaoting Zhang<sup>1†</sup>, Liguó Ding<sup>1†</sup>, Yongyao Yu<sup>1</sup>, Weiguang Kong<sup>1</sup>, Yaxing Yin<sup>1</sup>, Zhenyu Huang<sup>1</sup>, Xuezhen Zhang<sup>1</sup> and Zhen Xu<sup>1,2\*</sup>

## OPEN ACCESS

### Edited by:

Lluís Tort,

Autonomous University of Barcelona,  
Spain

### Reviewed by:

Hai-peng Liu,

Xiamen University, China

Felipe E. Reyes-López,

Autonomous University of Barcelona,  
Spain

### \*Correspondence:

Zhen Xu

zhenxu@mail.hzau.edu.cn

†These authors have contributed  
equally to this work

### Specialty section:

This article was submitted to  
Comparative Immunology,  
a section of the journal  
Frontiers in Immunology

Received: 30 July 2018

Accepted: 03 December 2018

Published: 18 December 2018

### Citation:

Zhang X, Ding L, Yu Y, Kong W, Yin Y,  
Huang Z, Zhang X and Xu Z (2018)  
The Change of Teleost Skin  
Commensal Microbiota Is Associated  
With Skin Mucosal Transcriptomic  
Responses During Parasitic Infection  
by *Ichthyophthirius multifiliis*.  
Front. Immunol. 9:2972.  
doi: 10.3389/fimmu.2018.02972

<sup>1</sup> Department of Aquatic Animal Medicine, College of Fisheries, Huazhong Agricultural University, Wuhan, China, <sup>2</sup> Laboratory for Marine Biology and Biotechnology, Qingdao National Laboratory for Marine Science and Technology, Qingdao, China

Teleost skin serves as the first line of defense against invading pathogens, and contain a skin-associated lymphoid tissue (SALT) that elicit gut-like immune responses against antigen stimulation. Moreover, exposed to the water environment and the pathogens therein, teleost skin is also known to be colonized by diverse microbial communities. However, little is known about the interactions between microbiota and the teleost skin mucosal immune system, especially dynamic changes about the interactions under pathogen infection. We hypothesized that dramatic changes of microbial communities and strong mucosal immune response would be present in the skin of aquatic vertebrate under parasite infection. To confirm this hypothesis, we construct an infected model with rainbow trout (*Oncorhynchus mykiss*), which was experimentally challenged by *Ichthyophthirius multifiliis* (Ich). H & E staining of trout skin indicates the successful invasion of Ich and shows the morphological changes caused by Ich infection. Critically, increased mRNA expression levels of immune-related genes were detected in trout skin from experimental groups using qRT-PCR, which were further studied by RNA-Seq analysis. Here, through transcriptomics, we detected that complement factors, pro-inflammatory cytokines, and antimicrobial genes were strikingly induced in the skin of infected fish. Moreover, high alpha diversity values of microbiota in trout skin from the experimental groups were discovered. Interestingly, we found that Ich infection led to a decreased abundance of skin commensals and increased colonization of opportunistic bacteria through 16S rRNA pyrosequencing, which were mainly characterized by lose of *Proteobacteria* and increased intensity of *Flavobacteriaceae*. To our knowledge, our results suggest for the first time that parasitic infection could inhibit symbionts and offer opportunities for other pathogens' secondary infection in teleost skin.

**Keywords:** mucosal immunity, skin, transcriptomic, microbiota, *Ichthyophthirius multifiliis*, rainbow trout (*Oncorhynchus mykiss*)

## HIGHLIGHTS

- Skin mucosal immunity interacts with the commensal microbiota that adhere to the epidermis.
- Parasitic infection leads to commensal microbial dysbiosis in trout skin.
- Successful invasion of Ich benefits the colonization of pathogens in teleost skin.
- Skin mucosal immunity can be activated by both parasitic infection and the subsequent infection caused by pathogens.

## INTRODUCTION

The skin of vertebrates serve as the first line of defense against pathogens' invading and harbor millions of microorganisms that form a very ancient and successful symbiosis between prokaryotes and metazoans. In all vertebrates, the skin shares a similar structure including two main layers (epidermis and dermis). In contrast to mammalian skin, teleost skin has been considered as mucosal surface that harbors abundant mucus-producing cells, lacks keratinization, and possesses living epithelial cells that make direct contact with the water medium (1, 2). Importantly, besides as one of important mucosal tissue, teleost skin has been discovered to contain a skin-associated lymphoid tissue (SALT) and elicit gut-like immune responses (3). Moreover, teleost skin is also known to be colonized by diverse microbial communities (4). The presence of bacterial communities in teleost skin also suggests a tight cross-talk between the microbiota and mucosal immune system. Although many studies have revealed the interaction between microbial communities and the host mucosal immune system of teleost fish (5–9), information regarding that in the skin remains limited (10).

As previously stated, the harmonious relationship between host and microbiota can be disrupted by pathogen infection, which lead to dysbiosis (11, 12). However, the distinction between a symbiont and pathogen is often blurry. Generally, symbionts are defined as microorganisms that induce anti-inflammatory cytokine expression in mucosal tissues, whereas pathogens induce pro-inflammatory responses (13, 14). Differently, in some cases, commensal will eventually trigger pro-inflammatory responses if present in high enough numbers (15). In addition, previous studies have shown that during the course of an infection, the relationships between the microbiota and the host's immune system are vulnerable to changes that render commensals into opportunists or pathogens (16), and largely impact the outcomes of infections (6). Thus, it's suggested that commensal microbiota play a fundamental role in mediating host–parasite interactions (9, 17, 18). Importantly, a number of studies have shed light on the changes in immune genes or bacterial communities at teleost mucosal sites after infection with different pathogens (16, 19, 20). Moreover, only few studies have taken advantage of the whole-transcriptome approach to investigate changes in immune gene expression in fish intestine, gills, skin, and olfactory organ (21–28). However, by far, almost no research has been performed to detect interactions

between the microbiota and the SALT of teleost during parasitic infections.

Here, using both the transcriptome and microbiome, our study examined the relationships between mucosal immunity and microbiota on the skin surfaces in teleost challenged with a parasite, *Ichthyophthirius multifiliis*, which poses the threat of serious economic loss to the worldwide trout farming industry (29). Our findings show that Ich successfully invading skin mucosa based on paraffin sections of skin stained with H & E. Moreover, we discover that the mucosal layer was destroyed by Ich, leading to heavy histopathological damage and microbial dysbiosis in trout skin. Importantly, significantly increased expression levels of numerous immune-related genes were discovered in trout skin after infection. In addition, the microbial dysbiosis in the skin of rainbow trout suggests that Ich has important inhibitory effects on commensals. Furthermore, our results show that skin mucosal immunity can be activated by both parasitic infection and the subsequent infection caused by opportunistic pathogens and pathogens. These results firstly demonstrate that the skin mucosal immune responses are associated with changed commensal microbiota after parasitic infection in teleost fish.

## MATERIALS AND METHODS

### Experimental Fish

Rainbow trout ( $10 \pm 1$  g) used in this study were obtained from fish farm in Shiyan (Hubei province, China), and maintained in aquarium tanks using a water recirculation system involving thermostatic temperature control and extensive biofiltration. Fish were acclimatized for at least 2 weeks at 15°C and fed with commercial trout pellets at a rate of 0.5–1% biomass twice a day (9:00 a.m. and 5:00 p.m.), and feeding was terminated 48 h prior to sacrifice. Animal procedures were approved by the Animal Experiment Committee of Huazhong Agricultural University and carried out according to the relative guidelines.

### Ich Parasite Isolation and Infection

The methods used for parasite isolation and infection were described previously by Xu et al with slight modification (30). Briefly, heavily infected rainbow trout were anesthetized with overdose of MS-222 and placed in a container with water to allow trophonts and tomites exit the host. The fish were taken out of the water after 4 h while the trophonts and tomites were left in the water at 15°C for about 24 h to let tomites formation and subsequent theront release.

For parasite infection, fish were exposed to an optimal single dose of ~5,000 theronts per fish added directly into the aquarium. Then tissue samples were taken after 12, 24, 48, 72 h, 7, 21, and 28 d (infected fish). Every experiment was performed at least three times. Control fish (mock infected) were maintained in a similar tank but without parasite. Fish were starved the days when sampling was conducted.

### Sample Collection

For sampling, rainbow trout were anesthetized with MS-222 and tissues were collected at the indicated time points after infection.

For histology and pathology study, a piece of the dissected skin ( $\sim 0.25 \text{ cm}^2$ ) under dorsal fin was clipped and immediately fixed in 4% (v/v) neutral buffered paraformaldehyde for at least 24 h. For RNA extraction and quantitative real-time PCR (qRT-PCR), tissue samples including skin, spleen and head kidney for all time points after infection were collected in sterile micro-centrifuge tubes. For 16S rRNA sequencing, skin samples from 24 h and 7 d post-infected fish and control fish were collected in sterile freezing tubes. All of these tissues collected for RNA or DNA analyses were immediately froze with liquid nitrogen and stored at  $-80^\circ\text{C}$  for further study.

## Histology, Light Microscopy, and Immunofluorescence Studies

After dissected and fixed in 4% neutral buffered formalin at  $4^\circ\text{C}$ , the trout skin tissues were then dehydrated in a graded ethanol series, cleaned in xylene, embedded in paraffin, and cut in sections of  $5 \mu\text{m}$  in duplicate with a rotary microtome (MICROM International GmbH, Germany). A copy of sections were stained with classical hematoxylin and eosin (H & E), while another portions were conventional stained with alcian blue (A & B). All the stained sections were examined under light microscope (Olympus, Japan). Quantification was performed by three different researchers.

Immunofluorescence staining was performed on paraffin sections obtained from the skin tissue of rainbow trout. For the detection of Ich parasite, paraffin sections were incubated overnight at  $4^\circ\text{C}$  with rabbit anti-Ich ( $0.2 \mu\text{g ml}^{-1}$ ) or its isotype control (rabbit IgG1 isotype;  $0.2 \mu\text{g ml}^{-1}$ ). After being washed three times with PBS (pH 7.2), samples were incubated for 2 h at  $20^\circ\text{C}$  with secondary antibody Alexa Flour<sup>®</sup> 488-AffiniPure goat anti-rabbit IgG (H + L; 115-545-003;  $2.5 \text{ mg ml}^{-1}$ , Jackson Scientific, Germany). Before mounting, all samples were stained with DAPI ( $4'$ , 6-diamidino-2-phenylindole;  $1 \text{ mg ml}^{-1}$ ; Invitrogen). Images were acquired and analyzed using Olympus BX53 fluorescence microscope (Olympus) and the iVision-Mac scientific imaging processing software (Olympus).

## RNA Isolation and Quantitative Real-Time PCR (qRT-PCR) Analysis

All the samples for quantitative real-time PCR (qRT-PCR) analyses were homogenized in 1 ml TRIZol (Invitrogen Life Technologies) using steel beads shaking (60 Hz for 1 min) and then subjected to total RNA extraction according to the manufacturer's instructions. The concentrations of the extracted RNA were quantified with a NanoDropND-1000 spectrophotometer (Thermo Scientific) and the integrity of the RNA was determined by agarose gel electrophoresis. To normalize gene expression levels for each sample, equivalent amounts of the total RNA ( $1 \mu\text{g}$ ) were incubated with RNase-free DNase I to eliminate contaminated genomic DNA. Then reverse transcription was performed using SuperScript first-strand synthesis system (Abm, Canada) in a  $20 \mu\text{l}$  reaction volume. The resultant cDNA was stored at  $-20^\circ\text{C}$ .

The relative expressions of immune-related genes were determined by qRT-PCR with each specific primer (Table 1).

The qRT-PCR were performed on a 7500 Real-time PCR system (Applied Biosystems, USA) using the EvaGreen  $2 \times$  qPCR Master mix (Abm, Canada). The total volume of qRT-PCR amplification system were  $10 \mu\text{l}$ , containing  $5 \mu\text{l}$  Master mix,  $1 \mu\text{l}$  diluted cDNA ( $300 \text{ ng}$ ),  $0.25 \mu\text{l}$  of each gene specific primer ( $10 \mu\text{M}$ ), and  $3.5 \mu\text{l}$  nuclease-free water. The internal control gene elongation factor  $1\alpha$  (EF1 $\alpha$ ) was employed as reference gene. To detect the relative abundance of Ich and *Flavobacterium columnare* (*F. columnare*), specie-specific 18S rRNA and 16S rRNA primers were used and shown in Table 1, respectively. All samples were performed as following conditions:  $95^\circ\text{C}$  for 30 s, followed by 40 cycles at  $95^\circ\text{C}$  for 1 s and at  $60^\circ\text{C}$  for 10 s. A dissociation protocol was carried out after thermos cycling to determine the specific-sized single application. Relative mRNA abundances were calculated using the  $2^{-\Delta\Delta\text{Ct}}$  method and normalized to EF1 $\alpha$ . The relative expression levels of immune-related genes were shown as  $2^{-\Delta\Delta\text{Ct}}$  while the relative abundance of Ich and *F. columnare* were shown as  $-\Delta\Delta\text{Ct}$  without further calculated to  $2^{-\Delta\Delta\text{Ct}}$ . All data were expressed as mean  $\pm$  standard error estimate (s. e. m.). Student's *t*-test was conducted using GraphPad 5.0. The results were obtained from three independent experiments and each was performed in triplicate.

## RNA-Seq Library Construction, Sequencing, and Analyses

The RNA samples of trout skin were sent to Novogene Bioinformatics Technology Co. Ltd. (Beijing, China), where the quality and quantity of total RNA were determined by a Nano Photometer spectrophotometer (IMPLEN, CA, USA), a Qubit 2.0 Fluorometer (Life Technologies, CA, USA), and a Agilent 2100 bioanalyzer (Agilent Technologies, CA, USA). Then the mRNA were purified by poly-T oligo-attached magnetic beads and fragmented by divalent cations in NEB Fragmentation Buffer. Random hexamer primers and M-MLV Reverse Transcriptase (RNase H) were used for first strand cDNA synthesis. Second strand cDNA synthesis was subsequently performed using DNA polymerase I and RNase H. These double-stranded cDNA fragments were end-repaired by adding a single "A" base and ligation of adapters. The adaptor modified fragments were selected by AMPure XP beads and amplified to create the final cDNA library. DGE sequencing was carried out on an Illumina NovaSeq platform that generated 150 bp paired-end raw reads.

Raw reads generated by paired-end sequencing were cleaned by removing sequences with Illumina adapters, filtering out reads with N and reads that half of the bases with a quality score below 20. Then the high-quality mRNA reads were mapped back to the *Oncorhynchus mykiss* genome ([ftp://ftp.ncbi.nlm.nih.gov/genomes/all/GCF/002/163/495/GCF\\_002163495.1\\_O-myk\\_1.0/](ftp://ftp.ncbi.nlm.nih.gov/genomes/all/GCF/002/163/495/GCF_002163495.1_O-myk_1.0/)) using Hisat2 (version 2.1.0) (31). Counts of each gene were extracted from the mapping files using Cufflinks (version 2.2.1) (32). Only the uniquely mapped genes which more than 10 reads in three or-more individual libraries were applied to differential expression genes' (DEGs) analyses using DESeq2 package (33). Finally, DEGs with adjusted  $P \leq 0.05$  and  $|\log_2(\text{fold-change})| \geq 1$  were considered as the targets for further analyses.

**TABLE 1** | Gene-specific primers used for quantitative real-time PCR in this study.

| Gene  | Primer                            | GenBank accession no. | Tm (°C) | Amplicon length (bp) | Primer Sequence (5'-3')    |                            |
|---|-----------------------------------|-----------------------|---------|----------------------|----------------------------|----------------------------|
|   |                                   |                       |         |                      | Forward primer             | Reverse primer             |
| <b>IMMUNOGLOBULINS AND THEIR RECEPTOR</b>   |                                   |                       |         |                      |                            |                            |
| IgT   | IgT-F/IgT-R                       | AY870264              | 58      |                      | CAGACAACAGCACCTCACCTA      | GAGTCAATAAGAAGACACAACGA    |
| IgM   | IgM-F/IgM-R                       | S63348.1              | 58      |                      | AAGAAAGCCTACAAGAGGGAGA     | CGTCAACAAGCCAAGCCACTA      |
| IgD   | IgD-F/IgD-R                       | AY748802.1            | 58      | 138                  | CAGGAGGAAAGTTCCGGCATCA     | CCTCAAGGAGCTCTGGTTTGA      |
| pIgR  | pIgR-F/pIgR-R                     | FJ940682.1            | 58      | 145                  | GTACAGCAGGTGTTACAGTAAC     | CCACAGACAGACCTTGATAAC      |
| <b>COMPLEMENT AND PATHWAY RELATED GENES</b> |                                   |                       |         |                      |                            |                            |
| Complement 3                                | C3-F/C3-R                         | XM_021561577.1        | 58      | 213                  | CCTCACAACAAGAGTGCACATC     | CCAAGTGGGCAAACCTCATCTCC    |
| Complement 1q-2                             | C1-F/C1-R                         | XM_021624859.1        | 58      | 176                  | TGAACAACCTGAACACCCC        | CAGCCTATTAGCCTGTAACCTCC    |
| Complement 7-1                              | C7-F/C7-R                         | NM_001124618.1        | 58      | 218                  | TATCTTCACTGCCACGGTC        | TAGCCTGTAACCTCCACATAGAC    |
| <b>CYTOKINES</b>                            |                                   |                       |         |                      |                            |                            |
| interleukin 2                               | IL2-F/IL2-R                       | AM422779.1            | 58      | 125                  | TGCTACAAGGAAACCCAA         | GCTGCAACAATGCAACTAT        |
| interleukin 11                              | IL11-F/IL11-R                     | NM_001124382.1        | 58      | 191                  | CAGAGCGTCAAGGAAACAC        | GCTCCTGGGAAGACTGTAA        |
| interleukin 22                              | IL22-F/IL22-R                     | AM 748537             | 58      | 101                  | GCAGGACAAGCATCATCCTAA      | CATTGTAGTGTTAATAGCACAGC    |
| interferon $\alpha$                         | IFN $\alpha$ -F/IFN $\alpha$ -R   | XM_021578986.1        | 58      | 180                  | CAGAGCCTCAGGAAGAACT        | CAAGGGGTAGAAGAGCATA        |
| IRF 1-2                                     | IRF1-F/IRF1-R                     | NP_001239293.1        | 58      | 173                  | CGAGACTACACCAGACCCTA       | TTGCTTTTGACCTCTTGTATT      |
| TNF $\alpha$                                | TNF $\alpha$ -F/TNF $\alpha$ -R   | XM_021576327.1        | 58      | 204                  | GTATGCGATGACACCTGAA        | GCCCCATTAGAGTGCCTTA        |
| CCL 19                                      | CCL19-F/CCL19-R                   | AIN40032.1            | 58      | 139                  | GTTTCCCTCGCCACTTCAA        | GCCACCCACTTGCTCTTTG        |
| <b>ICHTHYOPHTHIRIUS MULTIFILIIS</b>         |                                   |                       |         |                      |                            |                            |
| 18S rRNA                                    | Ic18-F/Ic18-R                     |                       | 60      |                      | AGTGACAAGAAATAGCAAGCCAGGAG | ACCCAGCTAAATAGGCAGAAGTTCAA |
| <b>FLAVOBACTERIUM COLUMNARE</b>             |                                   |                       |         |                      |                            |                            |
| 16S rRNA                                    | Fc16-F/Fc16-R                     | EU395796.1            | 60      | 146                  | GAGTGGCTAAGCGAAAGTGAT      | ACCTGACACCTCACGGCAC        |
| <b>REFERENCE GENE</b>                       |                                   |                       |         |                      |                            |                            |
| EF-1 $\alpha$                               | EF1-F/EF1-R                       | XM_021571866.1        | 58      |                      | CAACGATATCCGTCGTGGCA       | ACAGCGAAACGACCAAGAGG       |
| $\beta$ -actin                              | BA-F/BA-R                         | AB196465              | 60      | 225                  | CCGGCAGCTCACAGACTACC       | GTGCCATCTCCTGCTCAAA        |
| <b>OTHERS</b>                               |                                   |                       |         |                      |                            |                            |
| cathelicidin 1                              | CATH1-F/CATH1-R                   | NM_001124480.1        | 58      | 152                  | CTGGAGGCAAGCAACAAC         | CCCCAAGACGAGAGACA          |
| COL1 $\alpha$                               | COL1 $\alpha$ -F/COL1 $\alpha$ -R | NM_001124206.1        | 58      | 190                  | ATGTGCGACGAAGTGATTTG       | CGTTACCTGGAACACCCCTC       |
| m-csfr                                      | CSFR-F/CSFR-R                     | NM_001124739.1        | 58      | 120                  | CCCGCCTGTACCCCAATCT        | CGTCCCACCAATGCTTCT         |
| C-type lectin 4E                            | CTL4-F/CTL4-R                     | XM_021562202.1        | 58      | 137                  | GCAGCCACCTTACCATC          | CACCCATCTCCAATCCC          |
| DnajC3                                      | DC3-F/DC3-R                       | XM_021597283.1        | 58      | 166                  | TATTGAAACGTGTGTGGG         | AGGTGGTAGTAGATGGTGCTG      |
| DnajB9                                      | DB9-F/DB9-R                       | XM_021577464.1        | 58      | 234                  | CCGCTGTTGTTAGTGCTTT        | CGTCAGGACTCTTGTTCG         |
| ENO   | ENO-F/ENO-R                       | XM_021578347.1        | 58      | 214                  | TCAAGTCACTGACGACCC         | ACAGCCTGCTGGATACGC         |
| FHL1  | FHL1-F/FHL1-R                     | XM_021618853.1        | 58      | 212                  | CGGCTCTGAGAATGTGG          | ATGGCTGCTCCTGGTAG          |
| GAPDH                                       | GAPDH-F/GAPDH-R                   | NM_001124209.1        | 58      | 100                  | GACACCCACTCCTCCATCTT       | TGCTGTAGCCAAACTCATT        |
| LAMP3                                       | LAMP3-F/LAMP3-R                   | XM_021570344.1        | 58      | 211                  | TCAGGGTTCGGAGGTCGTA        | CACAGTGGGAAAGGAGTAA        |
| LDH   | LDH-F/LDH-R                       | XM_021605689.1        | 58      | 105                  | ACTCCAGCGTGCCCGTAT         | CGTGCTCCAGTCCCTCTT         |
| PFKA  | PFKA-F/PFKA-R                     | XM_021609920.1        | 58      | 103                  | CGACACCCGTTCCACAAT         | AGCCATCACAGCCTCCAC         |

The primers of IgT, IgM, and EF1 $\alpha$  were obtained from the previous study of Tacchi et al. (24).

## Bacterial 16S rRNA Sequencing and Taxonomic Analyses

When sampling materials for microbiota analysis, skin tissue together with mucus were taken in account. Skin pieces with mucus were collected and mixed from trout head above the gill cover, back of the body below the dorsal fin, belly under the lateral line, and end of the body in front of

the tail fin. About 200 mg skin sample was collected and homogenized by bead beating for 2 min at 60 Hz. Both fish and bacterial total genomic DNA were extracted following the manufacturer's recommendations of a DNA Min Kit (Qiagen, USA) and assessed photometrically using a NanoDrop ND-1000 spectrophotometer (Thermo Scientific). The universal primer set 515F (5' -GTGCCAGCMGCCGCGGTAA-3') and

806R (5'-GGACTACNNGGGTATCTAAT-3') was used for the amplification of the V4 hypervariable region of bacterial 16S rRNA genes. After preparation and generation, the 16S rRNA libraries were sequenced on Illumina HiSeq platform 2500 at Novogene Bioinformatics Technology Co., Ltd, Beijing, China.

The open-source software system Quantitative Insights into Microbial Ecology (QIIME) quality filters were used to conduct raw data (34). Then these filtered sequences in the samples were picked and clustered into operational taxonomic units (OTUs) at an identity threshold of 97%. Ribosomal Database Project (RDP) classifier was used for the taxonomic assignment. The number of OTUs present in the samples was determined and calculated the richness of Chao1 and indexes of Shannon diversity in species-level. Student's *t*-test was used to estimate differences in alpha diversity (observed species and Shannon index). The skin microbiota of each groups were defined and analyzed by identified the OTUs using eulerAPE (<http://www.eulerdiagrams.org/eulerAPE/>). Beta diversity and taxon composition were analyzed by QIIME for calculating both weighted and unweighted UniFrac (35). The weighted UniFrac phylogenetic distance metric was analyzed by Principal Coordinate Analysis (PCoA) to further visualize variations of community members and structure. We performed multiple response permutation procedure (MRPP) which provides a test of whether there is a significant difference between control and infected groups of sampling units. To find the biomarkers statistical significant among different groups, we present the linear discriminant analysis (LDA) effect size (LEfSe) method to support high dimensional class comparisons with a particular focus on metagenomic analysis. All statistical significance in this study was set at a  $P < 0.05$ .

## RESULTS

### Ich Infection Induced Morphological Changes and Immune Genes Expression in Trout Skin

To evaluate morphological changes and expressions of immune-related genes in the trout skin, we exposed fish to a parasite, *I. multifiliis* (Supplementary Figure 1A), which elicits strong immune responses in mucosal tissues such as skin and gills (3, 36). By H & E staining and anti-Ich antibody detection, Ich parasites were easily detected in the skin epidermis of trout after infection (Figures 1A,B). Besides, morphological changes were also observed in the skin epidermis of trout. Histological studies exhibited significant increase of both the thickness of the skin epidermis and the number of mucus cells in the trout skin after infection (Figures 1C,D). Interestingly, the thickness of trout skin epidermis was found to be significantly increased at 12 h post infection, and remained relative stable up to 28 d (Figure 1C). In addition, we discovered that a significantly increased number of mucus cells in skin epidermis occurred at 48 h after Ich infection, with a continued increase up to 28 d (Figure 1D and Supplementary Figure 2). Moreover, many white dots were seen on the trout skin at 7 d after infection (Supplementary Figure 1B). Similarly, we detected the

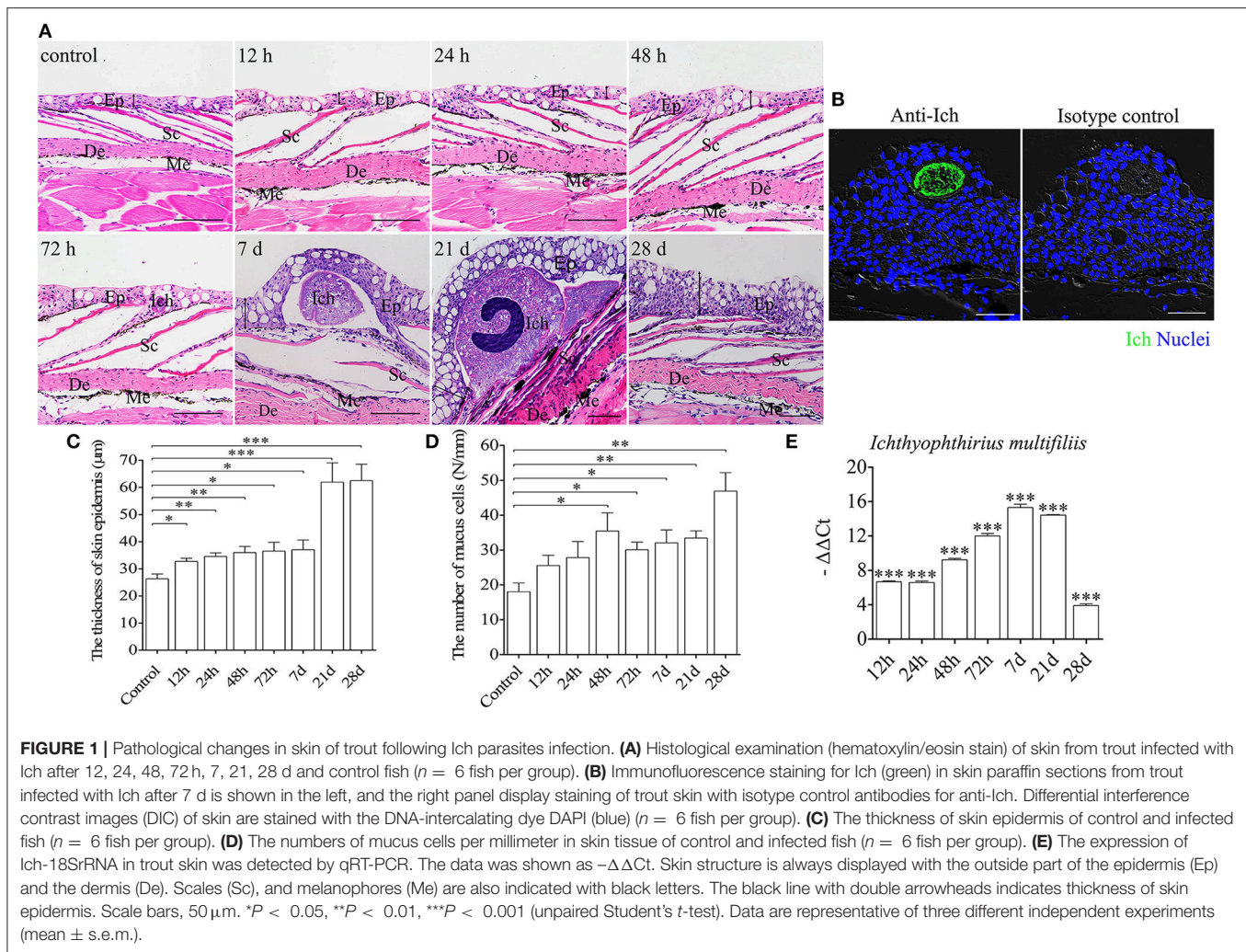
expression of Ich-18SrRNA in skin of trout after Ich infection and that of the control by qRT-PCR (Figure 1E). The result of high expression of Ich-18SrRNA in skin tissue further suggests that the parasite mainly succeeds in invading skin mucosal tissue.

To study the mRNA expression levels of immune-related genes and cell markers in trout skin after infection, we measured 12 immune-related genes including the cytokines (interleukin 2, 11 and 22; tumor necrosis factor  $\alpha$ , interferon  $\alpha$ , and interferon regulatory factor 1-2), chemokine gene (chemokine-like 19), complement 3 (C3), poly immunoglobulins receptor (pIgR), and immunoglobulin heavy chain genes (IgT, IgM, and IgD) (Figure 2A; primers used in this study are shown in Table 1) by qRT-PCR. Importantly, our studies discovered that strong immune responses occurred in the trout skin, head kidney, and spleen after challenge with Ich parasites. After infection, significantly up-regulated mRNA expressions of immune-related genes were detected in trout skin as early as 12 h (for IL22) or 24 h (IL2, IgT, IgM, and IgD) and reach their peak levels at 7 d, then recovered to control levels by 28 d (Figure 2B). While in the trout head kidney and spleen, delayed immune responses were discovered after challenge with Ich parasites, except TNF $\alpha$  at 48 h in head kidney and C3 at 12 h in spleen (Figure 2B). Interestingly, days 1 and 7 were the most relevant in terms of the intensity of the immune response in skin; therefore, these two time points were selected for subsequent RNA-Seq analysis.

### Analysis of Transcriptomic Changes in Trout Skin After Ich Infection

For further analysis of the two time points mentioned above, RNA-Seq libraries made from nine samples which separately represent three groups (control, E24h, and E7d) were sequenced on the Illumina platform. A total of 247,233,899 paired-end raw reads were generated. After filtration, 241,428,084 high-quality reads were harvested (Supplementary Table 1). The total clean reads were mapped back to *O. mykiss* sequences, and the mapped rate of each sample was over 80 percent (Supplementary Table 2). Unique mapped genes were further filtered, and only more than ten reads in three or-more individual libraries were used for differential expression genes (DEGs) analyses. As a result, the E24h/Con and E7d/Con groups yielded 27,536 and 27,692 valuable genes, respectively.

Prior to DEGs analysis, the filtered genes of each individual library were used to generate a PCA plot for principal component analysis (Figure 3A). As shown in the plot, there was a significant difference among the three treatment groups. During the statistical analysis, 1,745 DEGs were identified in the E24h/Con group (550 up-regulated and 1,195 down-regulated) and 4,357 DEGs in the E7d/Con group (1,721 up-regulated and 2,636 down-regulated). The distribution trends of DEGs in the pairwise comparisons (E24h/Con, E7d/Con) were presented as volcano plots (Figure 3B). From these plots, it is striking that there were much more up-regulated genes in the E7d than in the E24h group when compared with controls. After filtering by the *O. mykiss* immune gene library, more than 10 percent of DEGs indicated immune genes as shown in the Venn diagram (Figure 3B, right).

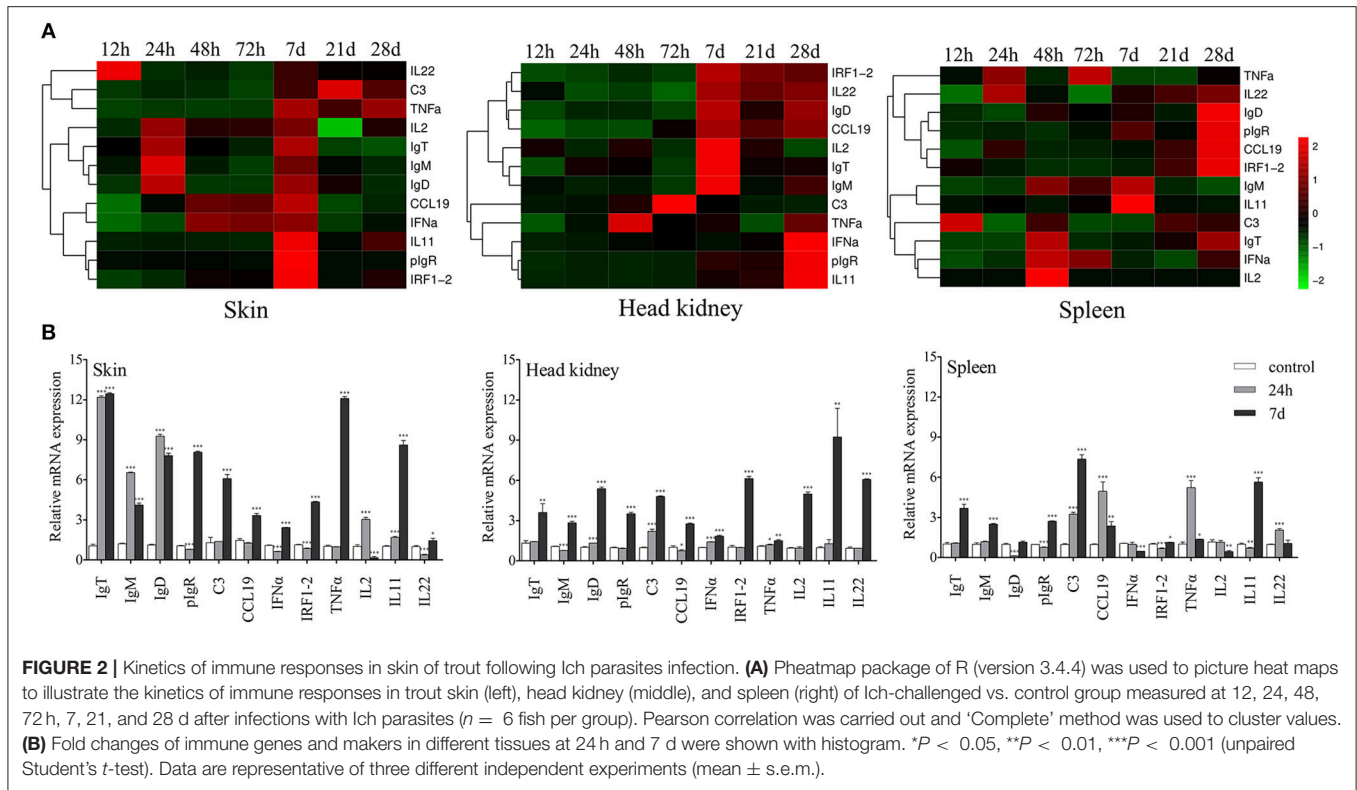


What is noteworthy is that 14.7% immune genes were only significantly up-regulated in the E7d/Con group, while 15.1% immune genes were significantly up-regulated at both time points. To validate the RNA-Seq expression levels, we randomly detected six up-regulated and six down-regulated immune genes' expression levels by qRT-PCR. The relative mRNA expression values determined by RNA-Seq and qRT-PCR were significantly correlated (**Figure 3D**), suggesting that RNA-Seq is as sensitive and accurate as qRT-PCR for determining gene expression *in vivo*.

Based on the common immune genes of the two aforementioned time points, we selected 20 genes with high differential expression. As shown in **Table 2**, most of the up-regulated immune genes belonged to innate immune molecules including lectin, mucins, pro-inflammatory cytokine, antimicrobial peptides, complement activation cytokines, and so on. In addition, complement and coagulation cascades as well as toll-like receptor (TLR) signaling pathways with their heat maps were generated to demonstrate the differential genes' expression patterns (**Figure 4** and **Supplementary Figure 3**, respectively). Interestingly, there is no significant change of

TLR expression. However, pro-inflammatory and chemotactic molecules (IL-1, IL-8) were up-regulated dramatically at both 24 h and 7 d. Moreover, some cytokines in connection with T cells (CD40, MIG) were also up-regulated markedly in the E7d/Con group. This indicates that adaptive immune response might be activated after 7 d post infection. Furthermore, almost all of the significantly different genes in complement and coagulation cascades pathways were up-regulated, suggesting that the complement components play a crucial role in anti-parasitic invasion.

To further investigate the DEGs which were involved in responding to Ich infection among the three groups, KEGG pathway enrichment analysis was conducted (37). As is shown in **Figure 3C**, both the signal transduction category and immune system category which were most related to immune response had an enormous advantage in gene count. In addition, 1,031 DEGs had KEGG Ortholog annotation; 618 DEGs had pathway annotation in the E24h/Con group, but only 7 pathways were significantly enriched ( $P < 0.001$ ), including complement and coagulation cascades pathways (**Supplementary Table 3**). In the E7d/Con group, 2,677 DEGs had KEGG Ortholog annotation,



1,582 DEGs had pathway annotation, and 33 pathways were significantly enriched ( $P < 0.001$ ) containing pathways associated with immune response, signal transduction, infectious disease, and cancer. Moreover, some protozoan parasite disease pathways were significantly enriched in the E7d/Con group, including amoebiasis and malaria (**Supplementary Table 3**). These results further suggest that the DEGs of the complement system play a crucial part in defense against parasite invasion and that a stronger immune response to Ich had occurred in the trout skin of E7d/Con group.

## 16S rRNA Sequencing and Taxonomic Analyses

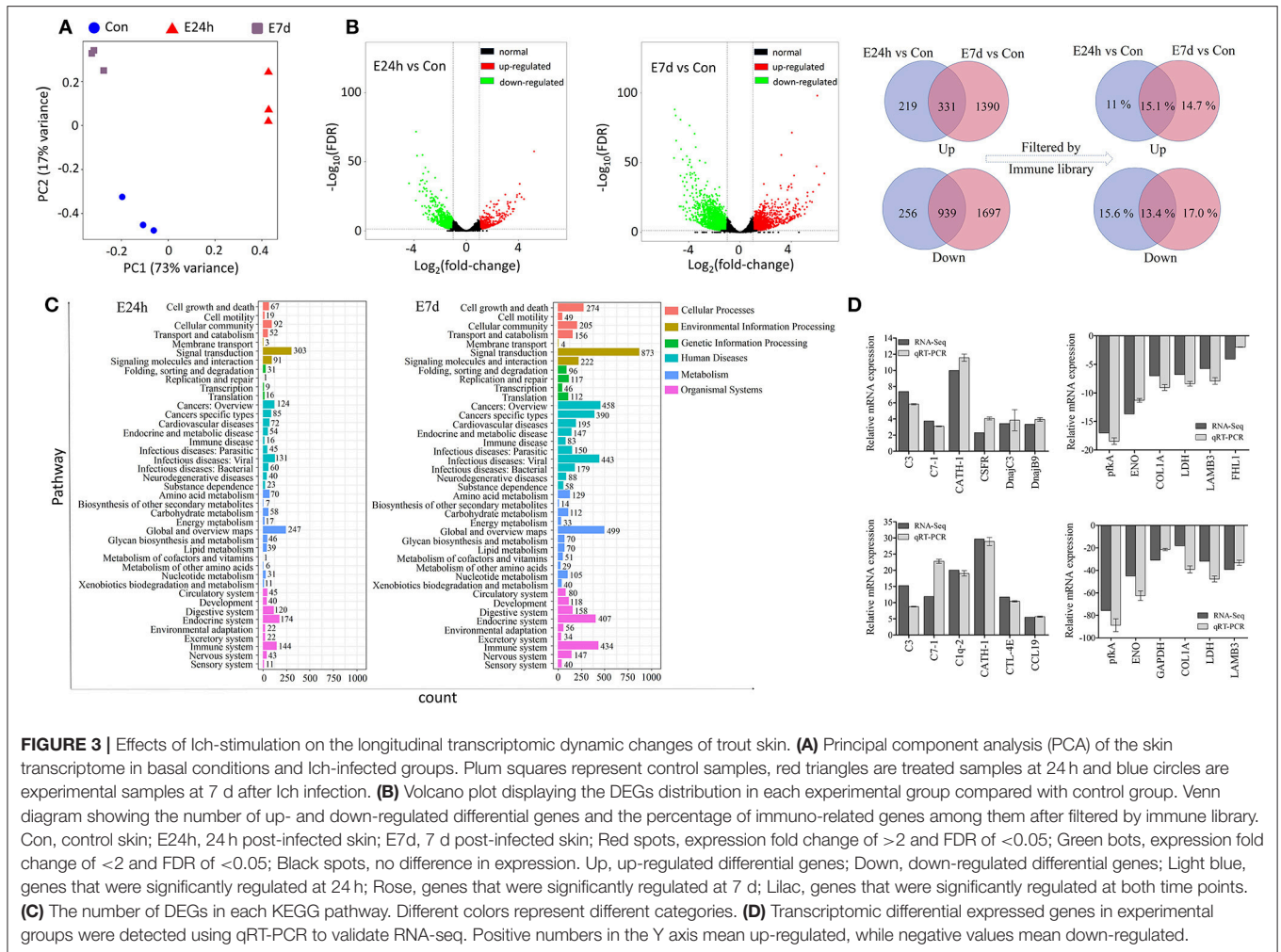
We investigated the abundance and diversity changes of trout skin microbiota communities in response to Ich infection using 16S rRNA sequencing of skin samples from control and infected fish by Illumina MiSeq run. We obtained 1,369,039 raw reads from the original samples collected at time intervals of 24 h and 7 d after Ich infection. Importantly, we developed a new protocol, facilitated by the Quantitative Insights Into Microbial Ecology (QIIME) toolkit (34), that can perform standard microbial community analysis techniques, including the quality filtering of reads, efficient operational taxonomic unit (OTU) picking, taxonomy assignment, the computation of  $\alpha$  and  $\beta$  diversity measures, and other analyses.

After the criteria filtering of raw reads, 1,293,982 high-quality clean reads were acquired in total and these were used for downstream analyses. The mean number of post-filter reads per sample was 76,057 that were exactly 252 nucleotides in length

respectively. The sequences were divided into unique OTUs at the 97% level using CD-HIT (38), which is the standard tool for this task when handling pyrosequencing data. Then 21,032 OTUs were noted and the total number of OTUs detected in experimental groups (E24h: 9,282 OTUs; E7d: 6,977 OTUs) were much higher than in the control groups (4,773 OTUs) of skin samples (**Supplementary Figure 4**). The data in our results indicated that the trout skin microbial community may have been altered by Ich infection.

## Ich Infection Results in Skin Microbial Dysbiosis

We calculated the differences in the microbial diversity and community in trout skin between the experimental and control groups by using the OTUs noted above for further analysis with UniFrac. Interestingly, high alpha diversity values of microbiota in trout skin from the experimental groups were discovered at both 24 h (Student's  $t$ -test,  $P = 0.0407$  for observed species and  $P = 0.0031$  for Shannon index) and 7 d ( $P = 0.0074$  for observed species and  $P = 0.0375$  for Shannon index) after Ich infection when compared with the control group (**Figure 5A**, **Table 3**). In addition, these changes were examined in beta diversity analysis using unweighted UniFrac and weighted UniFrac, and significant differences were observed at 24 h (**Figure 5B**, left for the unweighted UniFrac value) and 7 d (**Figure 5B**, right for the weighted UniFrac value). Thus, our result indicated that Ich infection could induce an increase of microbial diversity in trout skin.



We identified bacteria changes in Ich-infected individuals by classifying the phylum, class, order, family, and genus of the microbial sequences in trout skin from control and infected groups. The most abundant phyla across all samples were *Proteobacteria* followed by *Bacteroidetes*, *Firmicutes*, and *Actinobacteria* (Figure 5C). At the phylum level, the mean abundance of *Proteobacteria* dropped from 79% in control to  $56 \pm 3\%$  in infected groups. Meanwhile, the abundance of *Firmicutes* present increased from 1% in control fish to 14 and 7% in the 24 h and 7 d experimental groups, respectively. More importantly, an increased abundance (2.2-fold) of *Bacteroidetes* in trout skin was detected at 7 d after Ich infection. Additionally, the abundance of *Actinobacteria* was observed to increase (4.9-fold) as a result of Ich infection at 24 h (Figure 5C).

Details about the changes in the microbial community at the family and genus level were shown in a heat map for the top 35 abundant OTUs with significantly different abundances in each infected group (Figure 5D). Similar to the microbial abundance detected at the phyla level above, 12 OTUs, including the *Moraxellaceae*, *Shewanellaceae*, and *Pseudomonadaceae* family that belong to the phylum *Proteobacteria*, were detected with much higher abundances in the control group than the infected

groups. While in the E24h group, the phylum *Firmicutes* and *Actinobacteria* showed higher relative abundance than that in controls. Importantly, at seven days after Ich infection, the relative abundance of the family *Flavobacteriaceae* that belongs to *Bacteroidetes*, *Bdellovibrionaceae*, and *Rickettsiaceae* that belong to *Proteobacteria* were much higher than the other two groups.

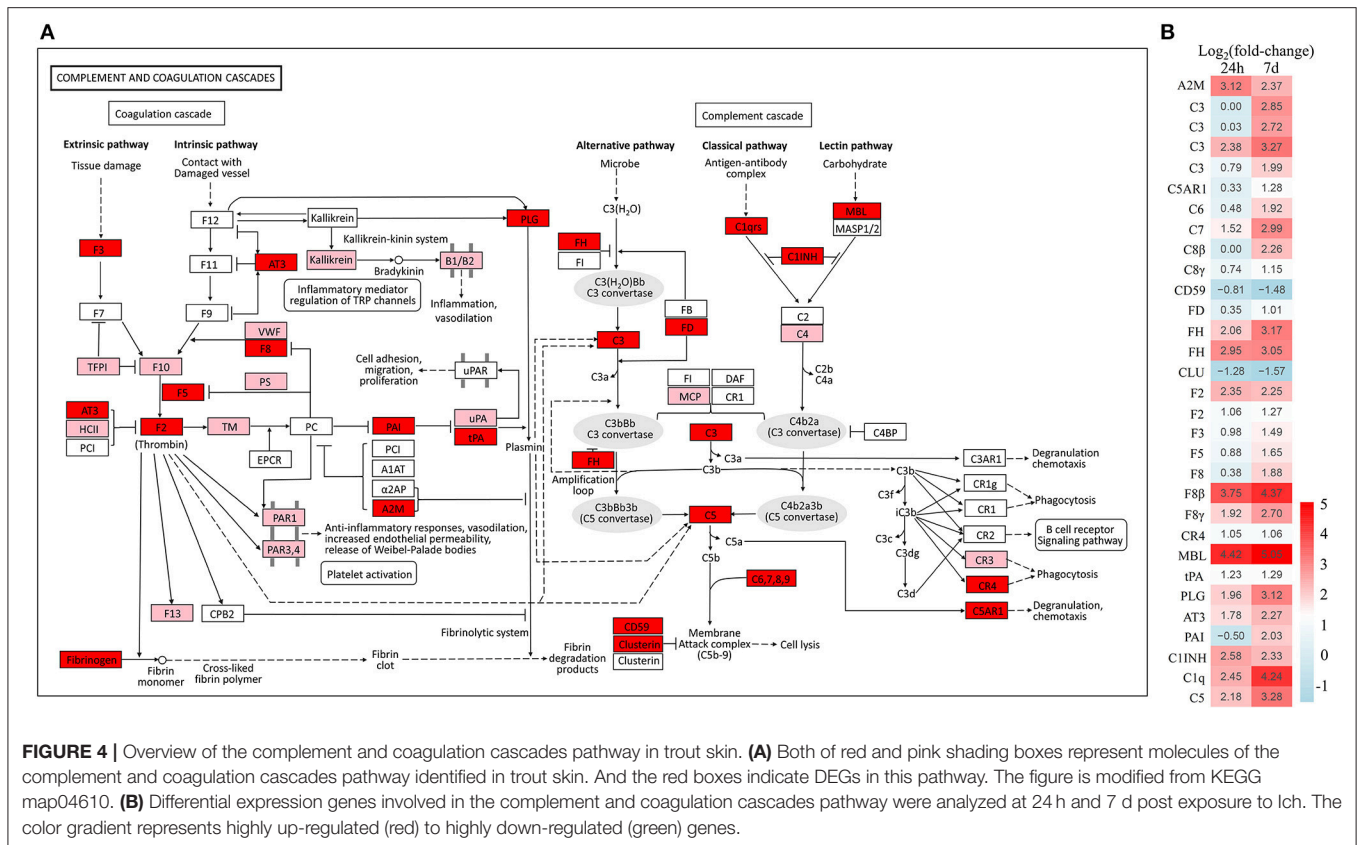
## Biomarkers of the Bacterial Community in Different Groups

Despite the findings that differences both of skin microbial communities' diversity and abundance were existed between the control group and experimental group, PCoA showed that Ich-infected samples clustered apart from each other and that the distances between control and infected groups were greater at 7 d than those at 24 h (Figure 6A). In addition, we determined whether Ich infection resulted in loss of important normal flora bacteria or increased opportunistic bacteria.

LDA Effect Size (LEfSe) analysis was used to further study the microbial biomarkers that contribute to the bacteria changes in different groups. Among the biomarkers, we observed that the abundances of *Acinetobacter* that belong

**TABLE 2** | The 20 up- and down- regulated immune genes.

| Gene name | GenBank accession no. | Description                        | E24h/Con |          | E7d/Con  |          |
|-----------|-----------------------|------------------------------------|----------|----------|----------|----------|
|           |                       |                                    | Log2FC   | FDR      | Log2FC   | FDR      |
| CATH-1    | NM_001124480.1        | Cathelicidin-1                     | 2.60740  | 8.18E-13 | 4.216072 | 1.81E-41 |
| Lectin    | NM_001124514.1        | Lectin                             | 3.25396  | 1.15E-16 | 6.180577 | 6.91E-35 |
| HP        | XM_021595153.1        | Hepcidin-like                      | -1.29474 | 0.003033 | 3.820614 | 7.83E-34 |
| APOA2     | NM_001161448.1        | Apolipoprotein A-II                | 3.857831 | 1.13E-15 | 4.087136 | 1.17E-34 |
| MMP13     | XM_021618131.1        | Collagenase 3                      | 0.988225 | 0.012413 | 4.02495  | 7.83E-33 |
| MRC       | XM_021588692.1        | Macrophage mannose receptor 1-like | 2.51501  | 1.04E-15 | 3.194697 | 2.43E-32 |
| HSP90α    | XM_021600916.1        | Heat shock protein HSP 90-alpha    | 1.682875 | 9.04E-09 | 3.337275 | 3.88E-21 |
| IL8       | XM_021625343.1        | permeability factor 2              | 1.017484 | 0.021847 | 2.845917 | 2.78E-16 |
| HP        | XM_021586023.1        | Haptoglobin-like                   | 3.282396 | 6.24E-18 | 4.183853 | 3.51E-16 |
| MUC-5AC   | XM_021607524.1        | Mucin-5AC-like                     | -1.36918 | 5.15E-05 | -2.72499 | 3.32E-15 |
| CTL       | XM_021562202.1        | C-type lectin                      | 0.874360 | 0.009486 | 2.939317 | 1.78E-15 |
| APOA1     | NM_001124247.1        | Apolipoprotein A-I                 | 4.075171 | 1.65E-27 | 3.613799 | 3.2E-13  |
| CFH       | NM_001124410.1        | Complement factor H                | 2.064596 | 1.17E-07 | 3.167978 | 1.45E-13 |
| C1q       | XM_021620193.1        | Complement C1q-like                | 2.453538 | 2.82E-06 | 4.240708 | 9.51E-11 |
| HSP90β    | NM_001124745.1        | Heat shock protein 70 beta         | 2.760112 | 1.38E-14 | 2.785039 | 1.5E-11  |
| CLEC4E    | NM_001160495.1        | C type lectin receptor beta        | 1.333084 | 0.000051 | 3.689057 | 2.57E-24 |
| MUC-2     | XM_021562134.1        | Mucin-2-like                       | 1.40047  | 0.001738 | -3.08191 | 5.23E-08 |
| MUC-5B    | XM_021580807.1        | Mucin-5B-like                      | 2.047236 | 0.000002 | 1.642672 | 0.00079  |
| RA        | XM_021604719.1        | Retinoic acid receptor responder   | -0.69702 | 0.200366 | -1.4504  | 0.001658 |
| MUC-17    | XM_021610915.1        | Mucin-17-like                      | 1.294894 | 0.008125 | 1.424968 | 0.010883 |



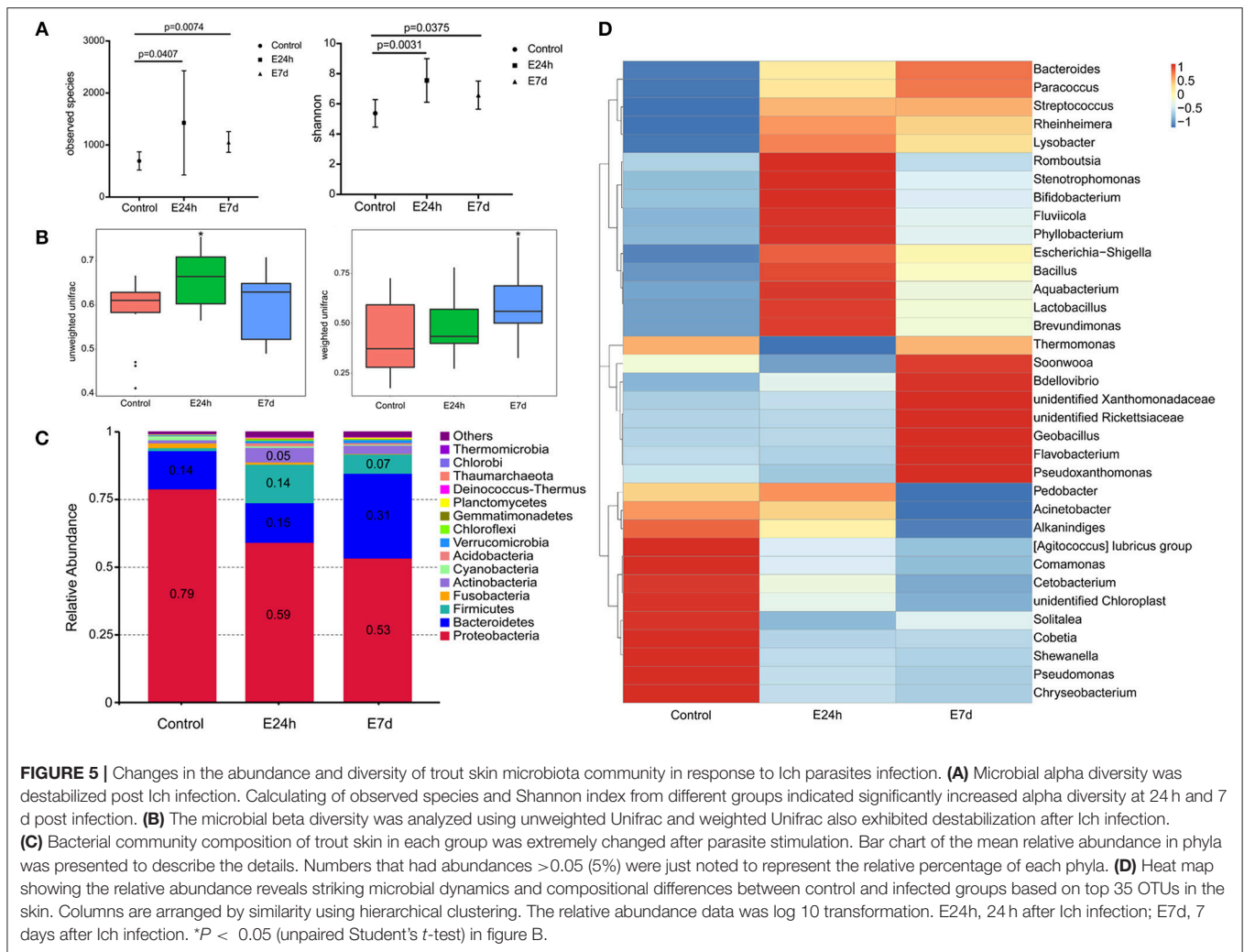


**TABLE 3 |** Alpha diversity metrics (mean  $\pm$  standard deviation) of the rainbow trout skin microbial community.

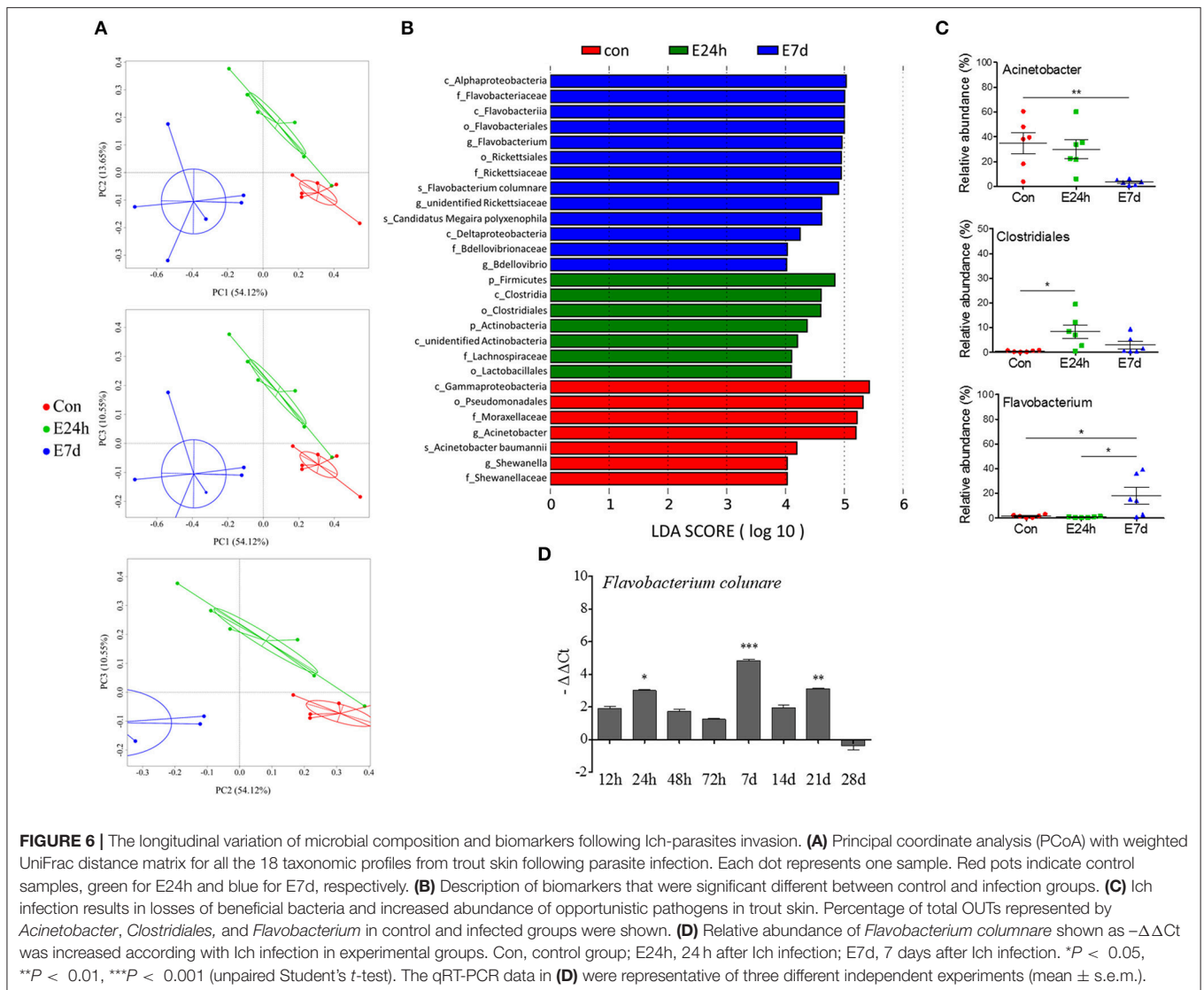
| Group | Observed species | Shannon | Simpson | Chao 1   | Ace      | Goods coverage | PD whole tree |
|-------|------------------|---------|---------|----------|----------|----------------|---------------|
| Con   | 694              | 5.372   | 0.92    | 870.29   | 883.019  | 0.995          | 69.198        |
| E24h  | 1,426            | 7.553   | 0.972   | 1579.935 | 1578.582 | 0.994          | 123.371       |
| E7d   | 1,050            | 6.582   | 0.932   | 1179.393 | 1175.885 | 0.996          | 100.089       |

to gammaproteobacteria phyla were significantly decreased at 7 d after infection (Figures 6B,C). Additionally, another two members of gammaproteobacteria phyla, which were the *Shewanella* and *Pseudomonas* genera were practically absent in infected samples (Supplementary Figure 5). In contrast, *Clostridiales*, *Actinobacteria*, and *Lachnospiraceae* scarcely existed in the control groups but were increased in the infected groups. We also found significantly increased abundances of *Flavobacterium*, *Rickettsiaceae*, and *Bdellovibrio* at 7 d after infection (Figure 6C, Supplementary Figure 5). Among the *Flavobacterium* members, *F. columnare* (*F. columnare*), which is well known as a bacterial pathogen that directly invades fish skin and gills and causes heavy infection, was significantly increased

in the skin microbial community of group E7d. Meanwhile, the relative abundance of *F. columnare* in trout skin was examined using qRT-PCR, and the increased presence of this pathogen was observed along with Ich infection (Figure 6D). However, it is difficult to detect both *F. columnare* (Figure 6D) and Ich (Figure 1E) in the trout skin from the control group. Taken together, our results first suggest that Ich parasite infection results in trout skin microbial dysbiosis.

## DISCUSSION

The skin is one of important mucosal surfaces and immune barriers in teleost fish, which represent the most ancient bony

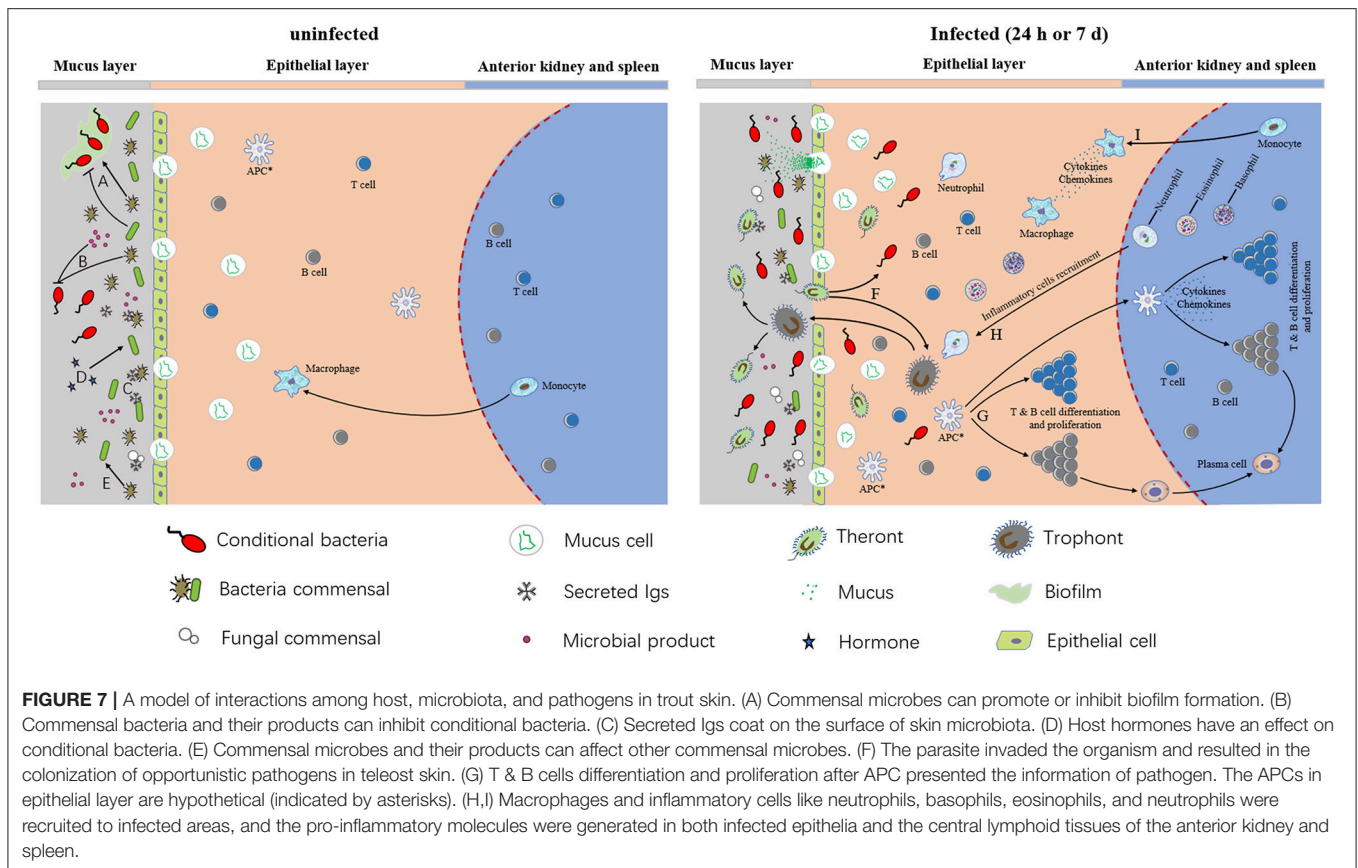


vertebrates that contain a SALT (3, 30). Due to the aquatic environment, the teleost skin surface coexists with millions of diverse microorganisms. Moreover, these microbiota and their products both directly and indirectly shape the skin mucosal system of teleost fish (39, 40). Although the interactions between commensal microbiota and the teleost mucosal immune system are known to be critical, however, the links between the teleost skin immune process and microbial dysbiosis after parasitic infection are poorly understood. To our knowledge, this study is the first time to show the transcriptome and microbiome in the skin of rainbow trout after challenged with the Ich parasites.

Here, we evaluate the pathological and morphological changes in trout skin after exposure to Ich. Although the entry route of Ich is currently unclear, we found the Ich parasite existed in the skin epidermis by H & E staining, which indicated that Ich has successfully invaded the trout skin mucosal tissue. With the occurrence of infection, significantly increased number of mucus

cells and thickness of epidermis were observed in trout skin. In agreement with the significant histopathological lesion in trout skin, we found that 12 immune-related genes were significantly activated in trout skin as early as 12 or 24 h when compared with those in head kidney and spleen after Ich infection. Our data probably suggest that teleost skin, as the first line to defense against Ich infection, activates the immune responses much earlier than that in systemic immune tissues such as head kidney and spleen. Importantly, at 7 d after infection, both the innate and adaptive immune molecules were responsive to Ich in trout skin. Future studies will investigate the specific contributions of adaptive immune molecules such as IgM, IgD, and IgT at the early stage to the skin immune response in teleost fish.

We used the next-generation sequencing based whole transcriptome analysis tool RNA-seq to characterize the details of all gene expression levels comprehensively at 24 h and 7 d in trout skin after Ich infection. The RNA-seq based expression studies provided a general view of the biological processes



that took place in the trout skin as a result of Ich infection. In total, 241,428,084 high-quality reads were harvested and mapped to unique locations in the *O. mykiss* sequences. By statistical analysis, we identified 1,745 DEGs in the E24h/Con group and 4,357 DEGs in the E7d/Con group. These data further suggest that the immune response of trout skin to Ich infection was stronger and more extensive in the E7d/Con than E24h/Con group according to the results we obtained by qRT-PCR. Importantly, our study has identified SALT-related immune molecules that respond to Ich, including cytokines, complement factors, and antibacterial peptides, all of which are known to be crucial in teleost's skin immune system. Below, we highlighted several key constituents of these categories and their potential functions in the context of trout skin responses to Ich.

Our RNA-Seq results showed increased expression levels of almost all significant DEGs in the complement pathway. As a bridge that connects innate and adaptive immunity in vertebrates, the complement system plays a pivotal role in the defense against pathogen invasion (41, 42). Previous study reported that the complement system of fish can be induced by either bacterial or parasitic infection (43, 44). In this study, 10 complement-related functional genes in total, including C1q, C3, C5, C6, C7, C8 $\beta$ , C8 $\gamma$ , MBL, FH, and FD, were activated following Ich infection in trout skin. Meanwhile, the membrane-bound complement regulatory protein (CD59) that acts to limit the assembly of membrane attack complex (MAC) and protects

the body's tissue cells from accidental damage by the complement system (45, 46), was significantly down-regulated in trout skin after challenge with Ich parasites. These results indicate that an intense response of complement factors to pathogens occurred in trout skin. Thus, the successful invasion of Ich both damaged the skin mucosal tissue and caused drastic reactions relating with complement in rainbow trout.

Moreover, our study found that the expression levels of pro-inflammatory cytokines (IL-1 $\beta$ , IL-8, and TNF- $\alpha$ ) were up-regulated after Ich infection. A previous study proved that cytokines are always produced at the pathogen entry site; they can drive inflammatory signals to regulate the capacity of residents and newly arrived phagocytes to destroy invading pathogens (47). As an important member of the pro-inflammatory cytokines, IL8 is barely noticeable in healthy tissues but can be rapidly induced by different inducers such as IL-1 $\beta$ , TNF- $\alpha$ , bacteria, viral products, and cellular stress (48, 49). Tumor necrosis factors (TNFs) are inflammatory cytokines that induce several immunological responses, including the apoptosis of infected cells (50). Combining previous studies, our results suggest that parasitic infection has induced drastic inflammatory reactions in trout skin.

In addition, other cytokines connected with T cells (CD40 and MIG) were also found to have markedly up-regulated expressions in the E7d/Con group while there was no significant change in TLR expression. Cytokines can also regulate antigen presentation

function in dendritic cells, and their migration to lymph nodes to initiate the adaptive immune response in mammals (47). Thus, we further speculate that Ich invasion may activate the adaptive immune system in trout skin.

Interestingly, significantly increased expression levels of antimicrobial peptides (hepcidin and cathelicidin-1) were detected in trout skin after parasite infection through RNA-Seq analysis. A previous study showed that hepcidin can protect grass carp against *F. columnare* infection via regulating the iron distribution and immune gene expressions (51). In teleost, cathelicidin can modulate the function of macrophages via the P2X7 receptor (52). We suppose that antimicrobial peptides (hepcidin and cathelicidin-1) may also play important roles in responding to parasite infection in trout skin. In addition, we hypothesize that the up-regulated genes here, which were previously proved to be mainly involved in antimicrobial immunity in teleost skin, are activated to combine with the increased bacterium after Ich infection.

In this study, we performed 16S rRNA sequencing that revealed important shifts in the skin bacterial community composition of rainbow trout in response to Ich infection. As mucus layer coated on fish skin is part of the skin associated mucosal system, fluctuations of the microbiota community load on trout skin and skin mucus were detected after Ich infection. We observed the differences of diversity indexes between the baseline skin microbiomes of Ich infected subjects and normal healthy individuals. In general, our data corroborate previous studies in terms of diversity changes after the pathogen infection (4, 16, 53). However, we found that the experimental groups had statistically significant higher values than the control group for the alpha diversity index, which was not absolutely identical to previous research (10). Interestingly, a recent study of Atlantic salmon showed no significant changes in the skin microbiome diversity (alpha diversity) of control and virus-infected fish due to high inter-individual variability (4). Moreover, increased diversity in the skin microbiome was observed in the evaluation of microbiota in both wild tropical fish skin and their parasitic loads (54). Thus, considering previous studies, our results indicate that the impact of pathogens on the fish microbiota diversity may vary between species and pathogens.

Previous study of Atlantic salmon indicated that fluctuations in environmental microbiota did not seem to be the root cause of skin microbiota differences after infected with salmon lice. Sampling point (time) as well as infection status are the drivers of microbiome community dynamics (53). Regarding community shifts, statistical analyses in our study similarly revealed that treatments and times after infection were important factors that could determine the composition of the skin microbial community in rainbow trout. *Proteobacteria* is the predominant phylum in the skin microbiome of teleost (10, 55, 56). The decrease of *Proteobacteria* abundance at 7 d after Ich infection in this study was primarily the result of the complete loss of *Acinetobacter*, a genus known to dominate the skin microbial community of trout. In addition, we discovered the absence of *Shewanella* and *Pseudomonas* of the *Proteobacteria* phylum in all Ich-infected groups regardless of infection time,

which indicates that these commensal bacterial species were unable to recolonize the host for the duration of the parasite infection. Importantly, several skin *Proteobacteria* isolates from salmonids have inhibitory effects against bacterial and fungal pathogen infections (10, 55). Moreover, *Proteobacteria* also dominate the human skin microbiome (57) and play a major role in the management of opportunistic bacteria regulating the host–environment relationship (58). Therefore, although the specific physiological contribution of *Proteobacteria* in the trout skin is currently unclear, further studies should investigate whether the decreased abundances of *Acinetobacter*, *Shewanella*, and *Pseudomonas* in *Proteobacteria* can contribute toward differences in the disease susceptibility of trout upon Ich infection.

In contrast to the decreased abundance of *Acinetobacter*, *Shewanella*, and *Pseudomonas*, we observed the increased incidence and intensity of *Flavobacterium* in trout skin after parasitic infection for the first time, particularly in the E7d experimental group of the present study. Our results parallel the previous study that *Aeromonas salmonicida* infection was associated with dominance shifting to opportunistic pathogens on the skin of Atlantic salmon (20). Similarly, the absence of the majority of the *Proteobacteria* and increased abundances of opportunistic bacterial pathogen (*Vibrionaceae*, *Flavobacteriaceae*, and *Streptococcaceae* sp.) were also detected in the skin of virus-infected salmon, which indicated that pathogen infection could facilitate colonization by opportunistic bacteria (4). These results agree with the observed expansions of *Flavobacteriaceae* and other known opportunistic taxa mentioned above in Ich-infected trout skin following lowered *Proteobacteria* abundance in our research. Thus, our results suggest that the increased abundance of *Flavobacteriaceae* could be opportunistic bacterium that may cause secondary infections in trout skin after parasite invasion. Besides, pathogens such as *F. columnare* were also proliferated due to Ich infection. Importantly, since our observations show a high presence of *F. columnare* in Ich-infected fish, there must be a link between Ich infection and *F. columnare* invasion in trout skin. As is shown in our study, Ich infection could cause mechanical damage in trout skin. We make a hypothesis that the skin damage augment the adhesion of secondary pathogenic bacteria to epithelial surfaces. Thus, Ich infection possibly provide opportunities for *F. columnare* adhesion.

In conclusion, our results summarize as a model that parasite infection, pathological changes, host mucosal immune responses, and bacterial community composition occur in the skin of rainbow trout. As shown in **Figure 7**, commensal microbes coexist in normal trout skin and play a key role in maintaining the homeostasis and suppression of the conditional bacteria. The continuously produced mucus layer covers trout skin and contain molecules with immunologically important properties, which interact directly with commensal microbial populations at skin surface. Besides, the interactions among different skin commensal bacteria are also benefit for maintaining the homeostasis. However, our study indicates that Ich infection destroyed both the homeostasis and the mucous layer. The

successful invasion of Ich results in significant histopathological lesions in trout skin, which in turn provide much more chances for Ich and other pathogens' infection. To deal with the disadvantage environment, mucus cells increased and released much more mucus to enhance physical or chemical barrier, and skin mucosal immune response are also induced at the same time. Our data first demonstrated that Ich infection results in dramatic immune responses, including inflammatory reactions, complement reaction, and bactericidal effects, and microbial dysbiosis, characterized most prominently by the decrease of *Proteobacteria* in trout skin. As for innate and adaptive immune response, studies of channel catfish and rainbow trout have shown that T and B cells are presented in fish skin and can respond to the protozoan parasite *I. multifiliis* infection (3, 59, 60). Neutrophils could surround the parasite *I. multifiliis* after 2–3 days post-infection and by 5–6 days inflammatory cells including neutrophils, eosinophils, and basophils can be recruited to infected areas of juvenile carp skin (61). In our study, pro-inflammatory cytokines such as IL8, IL-1 $\alpha$ , and TNF- $\beta$  are significantly up-regulated and these molecules play a role in the recruitment and maintenance of inflammatory cells in the rainbow trout skin after *I. multifiliis* infection (62). Furthermore, our results indicate that the loss of microbial balance caused by parasite infection likely impacts the health of the fish host, rendering the fish more susceptible to subsequent infections caused by the opportunistic pathogens and other bacterial pathogens present in the environment. These findings provide a critical basis for understanding the complexity of the interactions among pathogens, microbiota, and hosts in teleost fish. Future studies should address how the defensive mechanisms of specific immune responses in trout skin against Ich infection correlate with the observed changes in the skin microbiome of teleost fish.

## REFERENCES

- Schempp C, Emde M, Wolffe U. Dermatology in the darwin anniversary. part 1: evolution of the integument. *J Dtsch Dermatol Ges.* (2009) 7:750–7. doi: 10.1111/j.1610-0387.2009.07193.x
- Salinas I, Zhang YA, Sunyer JO. Mucosal immunoglobulins and B cells of teleost fish. *Dev Comp Immunol.* (2011) 35:1346–65. doi: 10.1016/j.dci.2011.11.009
- Xu Z, Parra D, Gomez D, Salinas I, Zhang YA, von Gersdorff Jorgensen L, et al. Teleost skin, an ancient mucosal surface that elicits gut-like immune responses. *Proc Natl Acad Sci USA.* (2013) 110:13097–102. doi: 10.1073/pnas.1304319110
- Reid KM, Patel S, Robinson AJ, Bu L, Jarungsriapisit J, Moore LJ, et al. Salmonid alphavirus infection causes skin dysbiosis in Atlantic salmon (*Salmo salar* L.) post-smolts. *PLoS ONE* (2017) 12:e0172856. doi: 10.1371/journal.pone.0172856
- Hooper LV, Midtvedt T, Gordon JI. How host-microbial interactions shape the nutrient environment of the mammalian intestine. *Annu Rev Nutr.* (2002) 22:283–307. doi: 10.1146/annurev.nutr.22.011602.092259
- Honda K, Littman DR. The microbiome in infectious disease and inflammation. *Annu Rev Immunol* (2012) 30:759–95. doi: 10.1146/annurev-immunol-020711-074937
- Ivanov II, Honda K. Intestinal commensal microbes as immune modulators. *Cell Host Microbe* (2012) 12:496–508. doi: 10.1016/j.chom.2012.09.009
- Maynard CL, Elson CO, Hatton RD, Weaver CT. Reciprocal interactions of the intestinal microbiota and immune system. *Nature* (2012) 489:231–41. doi: 10.1038/nature11551
- Chen TL, Chen S, Wu HW, Lee TC, Lu YZ, Wu LL, et al. Persistent gut barrier damage and commensal bacterial influx following eradication of *Giardia* infection in mice. *Gut Pathog* (2013) 5:26. doi: 10.1186/1757-4749-5-26
- Lowrey L, Woodhams DC, Tacchi L, Salinas I. Topographical mapping of the rainbow trout (*Oncorhynchus mykiss*) microbiome reveals a diverse bacterial community with antifungal properties in the skin. *Appl Environ Microbiol.* (2015) 81:6915–25. doi: 10.1128/AEM.01826-15
- Llewellyn MS, Boutin S, Hoseinifar SH, Derome N. Teleost microbiomes: the state of the art in their characterization, manipulation and importance in aquaculture and fisheries. *Front Microbiol.* (2014) 5:207. doi: 10.3389/fmicb.2014.00207
- Sylvain FE, Cheaib B, Llewellyn M, Gabriel Correia T, Barros Fagundes D, Luis Val A, et al. pH drop impacts differentially skin and gut microbiota of the Amazonian fish tambaqui (*Colossoma macropomum*). *Sci Rep.* (2016) 6:32032. doi: 10.1038/srep32032
- Nussbaum JC, Locksley RM. Infectious (non)tolerance-frustrated commensalism gone awry? *Cold Spring Harb Perspect Biol.* (2012) 4:a007328. doi: 10.1101/cshperspect.a007328
- Kaci G, Goudercourt D, Dennin V, Pot B, Doré J, Ehrlich SD, et al. Anti-inflammatory properties of *Streptococcus salivarius*, a commensal bacterium of the oral cavity and digestive tract. *Appl Environ Microbiol.* (2014) 80:928–34. doi: 10.1128/AEM.03133-13

## ETHICS STATEMENT

All animal procedures were approved by the Animal Experiment Committee of Huazhong Agricultural University (HZAUF1-2016-007) and carried out according to the relative guidelines.

## AUTHOR CONTRIBUTIONS

XiZ and LD performed most of the experiments, analyzed the data, and wrote the manuscript. YoY, WK, YaY, and ZH help with most of the experiments. XuZ contributed to setting up the Ich infection model. ZX designed the experiments and revised the manuscript. All authors reviewed the manuscript.

## FUNDING

This work was supported by grants from the National Natural Science Foundation of China (31873045), Huazhong Agricultural University Scientific and Technological Self-Innovation Foundation (2662016PY093) and The Thousand Youth Talents Program.

## ACKNOWLEDGMENTS

We thank Dr. J Oriol Sunyer (University of Pennsylvania) for help with experiments design and Dr. Jianguo Su (Huazhong Agriculture University) for critical reading of the manuscript.

## SUPPLEMENTARY MATERIAL

The Supplementary Material for this article can be found online at: <https://www.frontiersin.org/articles/10.3389/fimmu.2018.02972/full#supplementary-material>

15. Musharrafieh R, Tacchi L, Trujeque J, LaPatra S, Salinas I. *Staphylococcus warneri*, a resident skin commensal of rainbow trout (*Oncorhynchus mykiss*) with pathobiont characteristics. *Vet Microbiol.* (2014) 169:80–8. doi: 10.1016/j.vetmic.2013.12.012
16. Kelly C, Salinas I. Under pressure: interactions between commensal microbiota and the teleost immune system. *Front Immunol.* (2017) 8:559. doi: 10.3389/fimmu.2017.00559
17. Hayes KS, Bancroft AJ, Goldrick M, Portsmouth C, Roberts IS, Grecnis RK. Exploitation of the intestinal microflora by the parasitic nematode *Trichuris muris*. *Science* (2010) 328:1391–4. doi: 10.1126/science.1187703
18. Naik S, Bouladoux N, Wilhelm C, Molloy MJ, Salcedo R, Kastenmuller W, et al. Compartmentalized control of skin immunity by resident commensals. *Science* (2012) 337:1115–9. doi: 10.1126/science.1225152
19. Sigh J, Lindenstrøm T, Buchmann K. The parasitic ciliate *Ichthyophthirius multifiliis* induces expression of immune relevant genes in rainbow trout, *Oncorhynchus mykiss* (Walbaum). *J Fish Dis.* (2010) 27:409–17. doi: 10.1111/j.1365-2761.2004.00558.x
20. Cipriano RC, Dove A. *Far from Superficial: Microbial Diversity Associated with the Skin and Mucus of Fish[C]*. Khaled bin Sultan Living Oceans Foundation (2011). p. 156–7.
21. Micallef G, Bickerdike R, Reiff C, Fernandes JMO, Bowman AS, Martin SAM. Exploring the transcriptome of Atlantic Salmon (*Salmo salar*) skin, a major defense organ. *Mar Biotechnol.* (2012) 14:559–69. doi: 10.1007/s10126-012-9447-2
22. Long Y, Li Q, Zhou B, Song G, Li T, Cui Z. De novo assembly of mud loach (*Misgurnus anguillicaudatus*) skin transcriptome to identify putative genes involved in immunity and epidermal mucus secretion. *PLoS ONE* (2013) 8:e56998. doi: 10.1371/journal.pone.0056998
23. Xia JH, Liu P, Liu F, Lin G, Sun F, Tu R, et al. Analysis of stress-responsive transcriptome in the intestine of Asian Seabass (*Lates calcarifer*) using RNA-Seq. *DNA Res.* (2013) 20:449–60. doi: 10.1093/dnares/dst022
24. Tacchi L, Musharrafieh R, Larragoite ET, Crossey K, Erhardt EB, Martin SAM, et al. Nasal immunity is an ancient arm of the mucosal immune system of vertebrates. *Nat Commun.* (2014) 5:5205. doi: 10.1038/ncomms6205
25. Sun L, Liu S, Bao L, Li Y, Feng J, Liu Z. Claudin multigene family in channel catfish and their expression profiles in response to bacterial infection and hypoxia as revealed by meta-analysis of RNA-Seq datasets. *Comp Biochem Physiol Part D Genomics Proteomics* (2015) 13:60–9. doi: 10.1016/j.cbd.2015.01.002
26. Valenzuela-Miranda D, Boltaña S, Cabrejos ME, Yáñez JM, Gallardo-Escárate C. High-throughput transcriptome analysis of ISAV-infected Atlantic salmon *Salmo salar* unravels divergent immune responses associated to head-kidney, liver and gills tissues. *Fish Shellfish Immunol.* (2015) 45:367–77. doi: 10.1016/j.fsi.2015.04.003
27. Fatsini E, Bautista R, Manchado M, Duncan NJ. Transcriptomic profiles of the upper olfactory rosette in cultured and wild Senegalese sole (*Solea senegalensis*) males. *Comp Biochem Physiol Part D Genomics Proteomics* (2016) 20:125–35. doi: 10.1016/j.cbd.2016.09.001
28. Sun S, Ge X, Jian Z, Zhang W, Xuan F. De novo assembly of the blunt snout bream (*Megalobrama amblycephala*) gill transcriptome to identify ammonia exposure associated microRNAs and their targets. *Results Immunol.* (2016) 6:21–7. doi: 10.1016/j.rinim.2016.03.001
29. Ogut H, Akyol A, Alkan MZ. Seasonality of *Ichthyophthirius multifiliis* in the trout (*Oncorhynchus mykiss*) farms of the eastern black sea region of Turkey. *Turk J Fish Aquat Sci.* (2005) 5:23–7.
30. Xu Z, Takizawa F, Parra D, Gomez D, von Gersdorff Jorgensen L, LaPatra SE, et al. Mucosal immunoglobulins at respiratory surfaces mark an ancient association that predates the emergence of tetrapods. *Nat Commun.* (2016) 7:10728. doi: 10.1038/ncomms10728
31. Kim D, Langmead B, Salzberg SL. HISAT: a fast spliced aligner with low memory requirements. *Nat Methods* (2015) 12:357–60. doi: 10.1038/nmeth.3317
32. Trapnell C, Roberts A, Goff L, Pertea G, Kim D, Kelley DR, et al. Differential gene and transcript expression analysis of RNA-seq experiments with TopHat and Cufflinks. *Nat Protoc.* (2012) 7:562–78. doi: 10.1038/nprot.2012.016
33. Love MI, Huber W, Anders S. Moderated estimation of fold change and dispersion for RNA-seq data with DESeq2. *Genome Biol.* (2014) 15:550. doi: 10.1186/s13059-014-0550-8
34. Kuczynski J, Stombaugh J, Walters WA, Gonzalez A, Caporaso JG, Knight R. Using QIIME to analyze 16S rRNA gene sequences from microbial communities. *Curr Protoc Bioinformatics* (2011) Chapter 10, Unit 10.17. doi: 10.1002/0471250953.bi1007s36
35. Lozupone C, Lladser ME, Knights D, Stombaugh J, Knight R. UniFrac: an effective distance metric for microbial community comparison. *ISME J.* (2011) 5:169–72. doi: 10.1038/ismej.2010.133
36. Olsen MM, Kania PW, Heinecke RD, Skjoedt K, Rasmussen KJ, Buchmann K. Cellular and humoral factors involved in the response of rainbow trout gills to *Ichthyophthirius multifiliis* infections: molecular and immunohistochemical studies. *Fish Shellfish Immunol.* (2011) 30:859–69. doi: 10.1016/j.fsi.2011.01.010
37. Ogata H, Goto S, Sato K, Fujibuchi W, Bono H, Kanehisa M. KEGG: Kyoto encyclopedia of genes and genomes. *Nucleic Acids Res.* (1999) 27:29–34. doi: 10.1093/nar/27.1.29
38. Li W, Godzik A. Cd-hit: a fast program for clustering and comparing large sets of protein or nucleotide sequences. *Bioinformatics* (2006) 22:1658–9. doi: 10.1093/bioinformatics/btl158
39. Gomez D, Sunyer JO, Salinas I. The mucosal immune system of fish: the evolution of tolerating commensals while fighting pathogens. *Fish Shellfish Immunol.* (2013) 35:1729–39. doi: 10.1016/j.fsi.2013.09.032
40. Kanther M, Tomkovich S, Xiaolun S, Grosser MR, Koo J, Flynn EJIII, et al. Commensal microbiota stimulate systemic neutrophil migration through induction of serum amyloid A. *Cell Microbiol.* (2014) 16:1053–67. doi: 10.1111/cmi.12257
41. Mch H, Lambiris JD. The complement system in teleosts. *Fish Shellfish Immunol.* (2002) 12:399–420. doi: 10.1006/fsim.2001.0408
42. Nakao M, Tsujikura M, Ichiki S, Vo TK, Somamoto T. The complement system in teleost fish: progress of post-homolog-hunting researches. *Dev Comp Immunol.* (2011) 35:1296–308. doi: 10.1016/j.dci.2011.03.003
43. Dang Y, Xu X, Shen Y, Hu M, Zhang M, Li L, et al. Transcriptome analysis of the innate immunity-related complement system in spleen tissue of *Ctenopharyngodon idella* infected with *Aeromonas hydrophila*. *PLoS ONE* (2016) 11:e0157413. doi: 10.1371/journal.pone.0157413
44. Yin F, Gao Q, Tang B, Sun P, Han K, Huang W. Transcriptome and analysis on the complement and coagulation cascades pathway of large yellow croaker (*Larimichthys crocea*) to ciliate ectoparasite *Cryptocaryon irritans* infection. *Fish Shellfish Immunol.* (2016) 50:127–41. doi: 10.1016/j.fsi.2016.01.022
45. Huang Y, Qiao F, Abagyan R, Hazard S, Tomlinson S. Defining the CD59-C9 binding interaction. *J Biol Chem.* (2006) 281:27398–404. doi: 10.1074/jbc.M603690200
46. Wu G, Hu W, Shahsafaei A, Song W, Dobarro M, Sukhova GK, et al. Complement regulator CD59 protects against atherosclerosis by restricting the formation of complement membrane attack complex. *Circ Res.* (2009) 104:550–8. doi: 10.1161/CIRCRESAHA.108.191361
47. Bose M, Farnia P. Proinflammatory cytokines can significantly induce human mononuclear phagocytes to produce nitric oxide by a cell maturation-dependent process. *Immunol Lett.* (1995) 48:59–64. doi: 10.1016/0165-2478(95)02444-1
48. Abdelkhalik NK, Komiya A, Kato-Unoki Y, Somamoto T, Nakao M. Molecular evidence for the existence of two distinct IL-8 lineages of teleost CXC-chemokines. *Fish Shellfish Immunol.* (2009) 27:763–7. doi: 10.1016/j.fsi.2009.08.004
49. Perez-Cordon G, Estensoro I, Benedito-Palos L, Caldach-Giner JA, Sitja-Bobadilla A, Perez-Sanchez J. Interleukin gene expression is strongly modulated at the local level in a fish-parasite model. *Fish Shellfish Immunol.* (2014) 37:201–8. doi: 10.1016/j.fsi.2014.01.022
50. Savan R, Kono T, Igawa D, Sakai M. A novel tumor necrosis factor (TNF) gene present in tandem with the TNF- $\alpha$  gene on the same chromosome in teleosts. *Immunogenetics* (2005) 57:140–50. doi: 10.1007/s00251-005-0768-4
51. Wei X, Babu VS, Lin L, Hu Y, Zhang Y, Liu X, et al. Hepcidin protects grass carp (*Ctenopharyngodon idellus*) against *Flavobacterium columnare* infection via regulating iron distribution and immune gene expression. *Fish Shellfish Immunol.* (2018) 75:274–83. doi: 10.1016/j.fsi.2018.02.023
52. Li CH, Lu XJ, Li MY, Chen J. Cathelicidin modulates the function of monocytes/macrophages via the P2X7 receptor in a teleost, *Plecoglossus altivelis*. *Fish Shellfish Immunol.* (2015) 47:878–85. doi: 10.1016/j.fsi.2015.10.031

53. Llewellyn MS, Leadbeater S, Garcia C, Sylvain FE, Custodio M, Ang KP, et al. Parasitism perturbs the mucosal microbiome of Atlantic Salmon. *Sci Rep.* (2017) 7:43465. doi: 10.1038/srep43465
54. Hennesdorf P, Kleinertz S, Theisen S, Abdul-Aziz MA, Mrotzek G, Palm HW, et al. Microbial diversity and parasitic load in tropical fish of different environmental conditions. *PLoS ONE* (2016) 11:e0151594. doi: 10.1371/journal.pone.0151594
55. Boutin S, Bernatchez L, Audet C, Derome N. Antagonistic effect of indigenous skin bacteria of brook charr (*Salvelinus fontinalis*) against *Flavobacterium columnare* and *F. psychrophilum*. *Vet Microbiol.* (2012) 155:355–61. doi: 10.1016/j.vetmic.2011.09.002
56. Larsen A, Tao Z, Bullard SA, Arias CR. Diversity of the skin microbiota of fishes: evidence for host species specificity. *FEMS Microbiol Ecol.* (2013) 85:483–94. doi: 10.1111/1574-6941.12136
57. Cosseau C, Romano-Bertrand S, Duplan H, Lucas O, Ingrassia I, Pigasse C, et al. *Proteobacteria* from the human skin microbiota: species-level diversity and hypotheses. *One Health* (2016) 2:33–41. doi: 10.1016/j.onehlt.2016.02.002
58. Grice EA, Segre JA. The skin microbiome. *Nat Rev Microbiol.* (2011) 9:244–53. doi: 10.1038/nrmicro2537
59. Zhao X, Findly RC, Dickerson HW. Cutaneous antibody-secreting cells and B cells in a teleost fish. *Dev Comp Immunol.* (2008) 32:500–8. doi: 10.1016/j.dci.2007.08.009
60. Findly RC, Zhao X, Noe J, Camus AC, Dickerson HW. B cell memory following infection and challenge of channel catfish with *Ichthyophthirius multifiliis*. *Dev Comp Immunol.* (2013) 39:302–11. doi: 10.1016/j.dci.2012.08.007
61. Cross ML. Localized cellular responses to *Ichthyophthirius multifiliis*: protection or pathogenesis? *Parasitol. Today* (1994) 10:364. doi: 10.1016/0169-4758(94)90253-4
62. Buchmann K. Expression of pro-inflammatory cytokines in rainbow trout (*Oncorhynchus mykiss*) during an infection with *Ichthyophthirius multifiliis*. *Fish Shellfish Immunol.* (2004) 17:75–86. doi: 10.1016/j.fsi.2003.12.005

**Conflict of Interest Statement:** The authors declare that the research was conducted in the absence of any commercial or financial relationships that could be construed as a potential conflict of interest.

Copyright © 2018 Zhang, Ding, Yu, Kong, Yin, Huang, Zhang and Xu. This is an open-access article distributed under the terms of the Creative Commons Attribution License (CC BY). The use, distribution or reproduction in other forums is permitted, provided the original author(s) and the copyright owner(s) are credited and that the original publication in this journal is cited, in accordance with accepted academic practice. No use, distribution or reproduction is permitted which does not comply with these terms.